J Integral Finite Element Analysis for Three-Dimensional Cracks

Gein Wang*
East China Engineering Institute, Nanjing, China

In this paper a formulation of the J integral for three dimensional cracks in a centrifugal force field is presented The equations have been transformed into a form suitable for finite element method and a technique to simplify the resulting equations is presented The calculation of the J integral for the normal model with a semicircular surface crack at the center and an experiment with laser photoelasticity (stress freeze method) have been carried out under simple tensile loading The J integral calculation for a corner crack in an engine turbine disk has been performed taking the centrifugal force into account. The practical application demonstrates that the method presented in this paper is feasible and readily applicable

Nomenclature

u v and w	= displacements corresponding to the x y and z axes, respectively
x y z	= local coordinates
X Y Z	= global coordinates
u_i v_i, and w_i	= displacement at node i of the eight-node isoparametric element along the x y and z directions, respectively
γ_{ij}	= angular strain
ϵ_x, ϵ_y and ϵ_z	= strains corresponding to the x y and z axes, respectively
σ_{ij}	= component stress

Introduction

MANY cracks in rotating parts of the aircraft turbine engine are not penetrating and are three dimensional These parts function under the condition of a high centrifugal force field Therefore, it is necessary to study the problem of the three-dimensional crack in a centrifugal force field

Because the three dimensional J integral method has been selected, this method may use ordinary elements (eight-node and four node isoparametric elements) Refined meshes are not needed and the method of calculation presented in this paper is simple and convenient for practical application

The J integral for three dimensional cracks was given by Blackburn[1] in 1972 Centrifugal force was not then considered This formula has been extended in this study to include the effect of centrifugal force field

It is well known that the three dimensional formula is very complicated, even without consideration of centrifugal force Since an area integral is involved, many difficulties are encountered in its application The effect of the centrifugal force must also be taken into account. A technique for simplification and transformation is needed in order to transform the derived formula into a form suitable for the finite element method This paper presents a convenient method for simplifying the procedure In order to evaluate this method and program, some normal models (the ones for which computed results were available) have been calculated The calculation for a semicircular surface crack ($a=5$ mm) is accompanied by a laser photoelasticity experiment Finally, the value of the J integral for a corner crack existing at the bottom of a fir tree slot in the turbine disk is calculated.

The practical application has verified that the method presented in this paper is feasible and readily applicable

Formula of J Integral for Cracks in Centrifugal Force Field

The J integral formula for three dimensional cracks in a centrifugal force field has been derived and is given as:

$$J=\int_\Gamma (W\mathrm{d}y-T_i u_{i\,1}\mathrm{d}s)-\int_A (\sigma_{i3}u_{i\,1})_{\,3}\mathrm{d}A$$
$$-\int_A F_i u_{i\,1}\mathrm{d}A \qquad (1)$$

This formula is based on a coordinated system which consists of the principal normal, the binormal, and the tangent to the leading edge of the crack at the point where the J integral is to be performed (Fig 1a, point o) where $i=1, 2, 3$, corresponding to x y and z axes, respectively, and W is the density of strain energy, Γ is the path in xy plane, A is the area enclosed by the Γ path, T_i is the traction corresponding to direction i in the element ds on Γ path σ_{i3} is the stress corresponding to direction $i3$ at some point in the area A, u_i is the displacement corresponding to the direction i, i e , $u_1=u$ $u_2=v$ $u_3=w$ for conventional expression, and F_i is the centrifugal force per unit volume corresponding to the direction i

A brief derivation of Eq (1) is given as follows

First, a closed path in the xy plane (Fig 1b) is considered and let

$$\Gamma_p=\int_\Gamma (W\mathrm{d}y-T_i u_{i\,1}\mathrm{d}s) \qquad (2)$$

Substituting the boundary conditions

$$T_x=\sigma_x\cos(n\ x)+\sigma_{xy}\cos(n\ y)+\sigma_{xz}\cos(n\ z) \qquad (3a)$$

$$T_y=\sigma_{xy}\cos(n,\ x)+\sigma_y\cos(n\ y)+\sigma_{yz}\cos(n\ z) \qquad (3b)$$

$$T_z=\sigma_{zx}\cos(n\ x)+\sigma_{zy}\cos(n\ y)+\sigma_z\cos(n\ z) \qquad (3c)$$

Received June 11, 1982; presented as Paper 82 1060 at the AIAA/SAE/ASME 18th Joint Propulsion Conference Cleveland Ohio June 21 23 1982; revision received Nov 19 1983

*Instructor and Head of Material Mechanics Laboratory

into Eq (2) and noting that

$$\cos(n\ z) = \cos 90\ \text{deg} = 0$$

gives

$$\Gamma_p = \int_{\Gamma^*} \left\{ W\mathrm{d}y - \left[\left(\sigma_x \frac{\partial u}{\partial x} + \sigma_{xy} \frac{\partial v}{\partial x} + \sigma_{zx} \frac{\partial w}{\partial x} \right) \mathrm{d}y - \left(\sigma_{xy} \frac{\partial u}{\partial x} + \sigma_y \frac{\partial v}{\partial x} + \sigma_{zy} \frac{\partial w}{\partial x} \right) \mathrm{d}x \right] \right\} \tag{4}$$

According to Green's theorem

$$\Gamma_p = \int_{A1} \left\{ \frac{\partial w}{\partial x} - \left[\frac{\partial}{\partial x} \left(\sigma_x \frac{\partial u}{\partial x} + \sigma_{xy} \frac{\partial v}{\partial x} + \sigma_{zx} \frac{\partial w}{\partial x} \right) + \frac{\partial}{\partial y} \left(\sigma_{xy} \frac{\partial u}{\partial x} + \sigma_y \frac{\partial v}{\partial x} + \sigma_{zy} \frac{\partial w}{\partial x} \right) \right] \right\} \mathrm{d}x\mathrm{d}y \tag{5}$$

Substituting

$$\epsilon_x = \partial u/\partial x \tag{6a}$$

$$\epsilon_y = \partial v/\partial y \tag{6b}$$

$$\epsilon_z = \partial w/\partial z \tag{6c}$$

$$\gamma_{xy} = \partial v/\partial x + \partial u/\partial y \tag{6d}$$

$$\gamma_{yz} = \partial w/\partial y + \partial v/\partial z \tag{6e}$$

$$\gamma_{zx} = \partial u/\partial z + \partial w/\partial x \tag{6f}$$

and

$$2W = \sigma_x \epsilon_x + \sigma_y \epsilon_y + \sigma_z \epsilon_z + \sigma_{xy} \gamma_{xy} + \sigma_{yz} \gamma_{yz} + \sigma_{zx} \gamma_{zx} \tag{7}$$

into Eq (5) gives

$$\Gamma_p = \int_{A1} \left\{ \frac{\partial}{\partial z} \left(\sigma_z \frac{\partial w}{\partial x} + \sigma_{yz} \frac{\partial v}{\partial x} + \sigma_{zx} \frac{\partial u}{\partial x} \right) - \left[\frac{\partial u}{\partial x} \left(\frac{\partial \sigma_x}{\partial x} + \frac{\partial \sigma_{xy}}{\partial y} + \frac{\partial \sigma_{zx}}{\partial z} \right) + \frac{\partial v}{\partial x} \left(\frac{\partial \sigma_{xy}}{\partial x} + \frac{\partial \sigma_y}{\partial y} + \frac{\partial \sigma_{yz}}{\partial z} \right) + \frac{\partial w}{\partial x} \left(\frac{\partial \sigma_{zx}}{\partial x} + \frac{\partial \sigma_{zy}}{\partial y} + \frac{\partial \sigma_z}{\partial z} \right) \right] \right\} \mathrm{d}x\mathrm{d}y \tag{8}$$

From the equilibrium equations

$$\partial \sigma_x/\partial x + \partial \sigma_{xy}/\partial y + \partial \sigma_{xz}/\partial z - \rho \partial^2 u/\partial t^2 = 0 \tag{9a}$$

$$\partial \sigma_{yz}/\partial x + \partial \sigma_y/\partial y + \partial \sigma_{yz}/\partial z - \rho \partial^2 v/\partial t^2 = 0 \tag{9b}$$

$$\partial \sigma_{zx}/\partial x + \partial \sigma_{zy}/\partial y + \partial \sigma_z/\partial z - \rho \partial^2 w/\partial t^2 = 0 \tag{9c}$$

where ρ is density and t is time

Letting

$$F_x = -\rho\ \partial^2 u/\partial t^2$$

$$F_y = -\rho\ \partial^2 v/\partial t^2 \quad F_z = -\rho\ \partial^2 w/\partial t^2$$

and adding to and subtracting from the right side of Eq (8) the expression

$$\int_{A1} (\partial u/\partial x\ F_x + \partial v/\partial x\ F_y + \partial_w/\partial_x\ F_z)\,\mathrm{d}x\mathrm{d}y$$

the following equation can be obtained

$$\Gamma_p = \int_{A1} \frac{\partial}{\partial z} \left(\sigma_z \frac{\partial w}{\partial x} + \sigma_{yz} \frac{\partial v}{\partial x} + \sigma_{xz} \frac{\partial u}{\partial x} \right) \mathrm{d}x\mathrm{d}y + \int_{A1} \left(\frac{\partial u}{\partial x} F_x + \frac{\partial v}{\partial x} F_y + \frac{\partial w}{\partial x} F_z \right) \mathrm{d}x\mathrm{d}y \tag{10}$$

Substituting Eq (2) into Eq (10) and subtracting the expression

$$\left[\int_{A2} \frac{\partial}{\partial z} \left(\sigma_z \frac{\partial w}{\partial x} + \sigma_{yz} \frac{\partial v}{\partial x} + \sigma_{xz} \frac{\partial u}{\partial x} \right) \mathrm{d}x\mathrm{d}y + \int_{A2} \left(\frac{\partial u}{\partial x} F_x + \frac{\partial v}{\partial x} F_y + \frac{\partial w}{\partial x} F_z \right) \mathrm{d}x\mathrm{d}y \right]$$

from the right and left sides of the equation, also noting that when the pressure of the gas on crack surface is neglected, the contribution to Γ3 and Γ4 (Fig 1c) is zero and the following

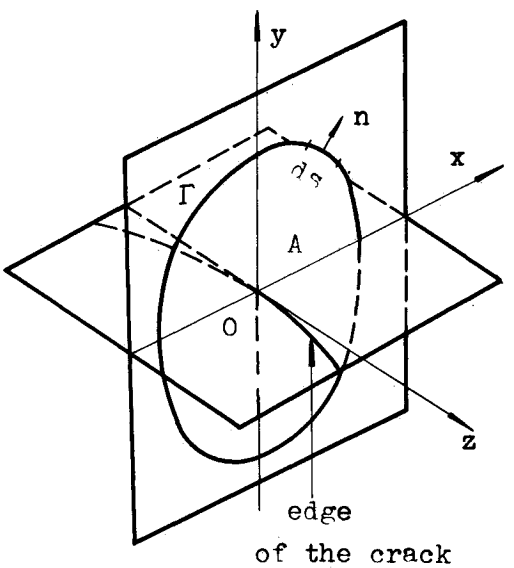

Fig 1a Coordinate system

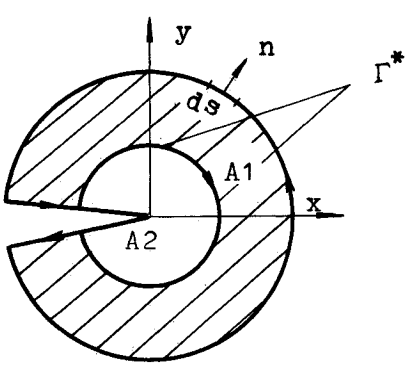

Fig 1b Closed path.

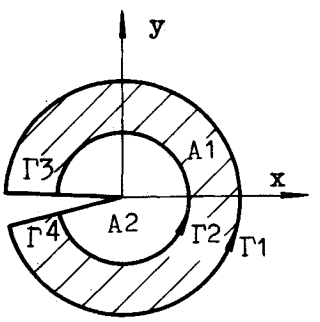

Fig 1c Name of each part of the path

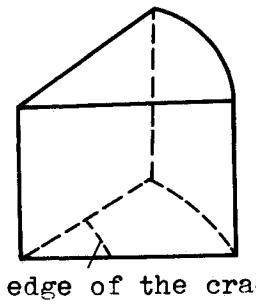

Fig 2a Pattern model

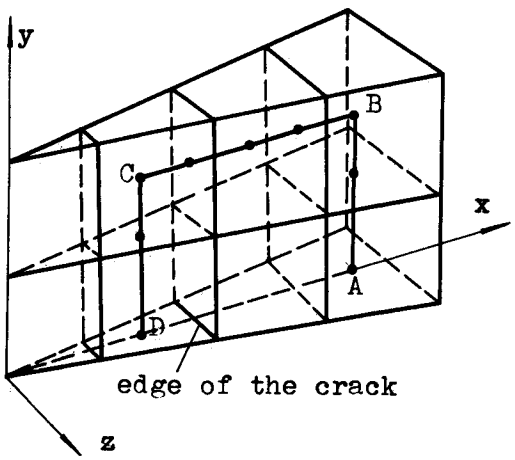

Fig 2b Path of the integral

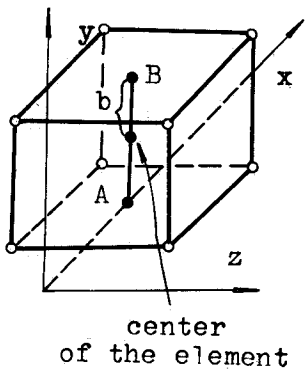

Fig 2c Line integral along *y* direction

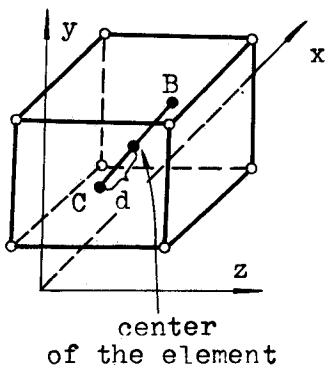

Fig 2d Line integral along *x* direction

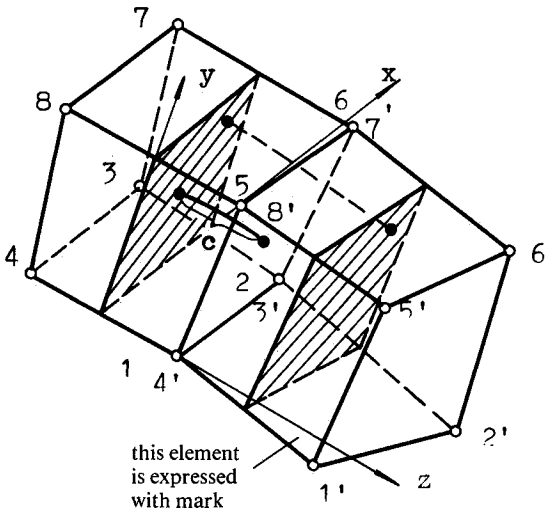

Fig 2e First area integral in formula (1)

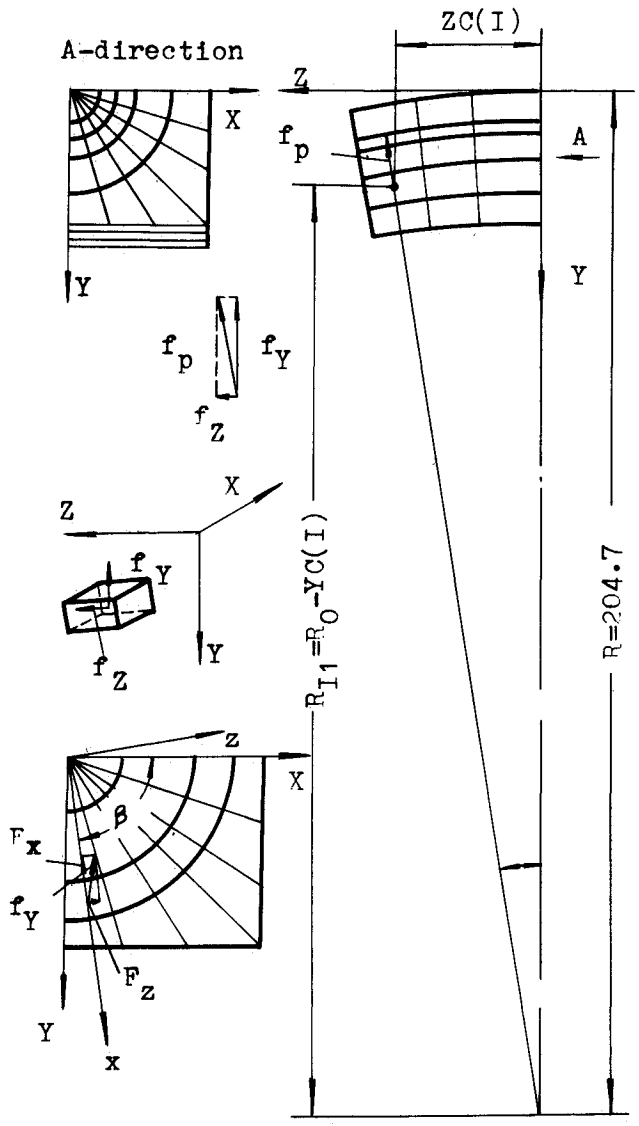

Fig 2f Calculation of centrifugal force

equation is obtained

$$\int_{\Gamma 1}(W\mathrm{d}y - T_i u_{i,1}\mathrm{d}s) - \int_{(A1+A2)}\frac{\partial}{\partial z}\left(\sigma_z\frac{\partial w}{\partial x}+\sigma_{yz}\frac{\partial v}{\partial x}+\sigma_{xz}\frac{\partial u}{\partial x}\right)\mathrm{d}x\mathrm{d}y - \int_{(A1+A2)}\left(F_x\frac{\partial u}{\partial x}+F_y\frac{\partial v}{\partial x}+F_z\frac{\partial w}{\partial x}\right)\mathrm{d}x\mathrm{d}y = \int_{\Gamma 2}(W\mathrm{d}y - T_i u_{i,1}\mathrm{d}s) - \int_{A2}\frac{\partial}{\partial z}\left(\sigma_z\frac{\partial w}{\partial x}+\sigma_{yz}\frac{\partial v}{\partial x}+\sigma_{xz}\frac{\partial u}{\partial x}\right)\mathrm{d}x\mathrm{d}y - \int_{A2}\left(F_x\frac{\partial u}{\partial x}+F_y\frac{\partial v}{\partial x}+F_z\frac{\partial w}{\partial x}\right)\mathrm{d}x\mathrm{d}y$$

Since the path is selected arbitrarily, it is evident that an invariable exists If this invariable is denoted by J, then

$$\mathrm{J}=\int_{\Gamma}(W\mathrm{d}y - T_i u_{i,1}\mathrm{d}s) - \int_A(\sigma_{i3}u_{i,1})_{,3}\mathrm{d}A - \int_A F_i u_{i,1}\mathrm{d}A$$

When the centrifugal force is neglected, formula (1) presented in this paper becomes the same as that given by Miyamoto [2] If only the two-dimensional case is considered, it turns out to be the one given by Sakata [3]

Finite Element Formulation

It is evident that using Eq (1) directly to solve the problems with the arbitrary crack model is very difficult and tedious, and that a simplified technique is desirable to make it suitable for engineering application In this section, such a simplified technique for transforming formula (1) into a form suitable for finite element formulation is presented To sum up, this technique of simplification means using the "pattern model" in the J integral area near the leading edge of the crack and letting the integral path pass through the center of the elements A "pattern model" is the sector model ¼ cylinder, or semicylinder, etc as shown in Fig 2a Passing through the center means that an integral path is chosen for the "pattern model" so that it may pass through the center of corre sponding elements (Fig. 2b)

A question arises naturally: since the models of the three dimensional crack are variable, how can they be related to those "pattern models"? It is noted that the basic coordinate system of formula (1) consists of the principal normal, the binormal, and the tangent to the edge of the crack at the point where J is to be determined For any point on an arbitrary space curve, there exists a tangent plane, and, naturally, a curvature radius This provides us with the theoretical basis that relates an arbitrary crack model with the "pattern model," i e , for any crack we then can redivide the mesh so that the small area near the leading edge of the crack is composed of the "pattern model." The elements of the pattern model may cause many terms of the Jacobian matrix to vanish because of their symmetry Moreover, since the integral path passes through the center of the elements, many additional terms may also vanish The process of the calculation is greatly simplified Consequently, complicated formula (1) can be readily used in engineering calculation. In practice, the procedure consists first in calculating the five parameters, i e , *WSI* *AB(1)* *AB(2)* *ABC* and *ABC2* for each element The parameter *WSI* reflects the density of the strain energy; *AB(1)* and *AB(2)* reflect $T_i u_i, {}_1\mathrm{d}s$ in the first integral of formula (1); *ABC*, the value in the second integral, and *ABC2*, the value in the third integral of formula (1) i e , the effect of the centrifugal force These parameters are then stored in memories for further use When the J integral is to be performed they are found out and combined in terms of various needs The details for deriving these five parameters are not given here Only the results are given below From them, it is evident that the determination of these parameters is quite simple

1) *AB*(1) is the parameter representing the line integral along *AB*(Fig 2c) and can be expressed as

$$AB(1)=(\sigma_x\ PP+\sigma_{xy}\cdot QQ+\sigma_{xz}\ RR)\ b/4d \tag{11}$$

where

$$PP=-u_1+u_2+u_3-u_4-u_5+u_6+u_7-u_8 \tag{12a}$$

$$QQ=-v_1+v_2+v_3-v_4-v_5+v_6+v_7-v_8 \tag{12b}$$

$$RR=-w_1+w_2+w_3-w_4-w_5+w_6+w_7-w_8 \tag{12c}$$

and *b* and *d* are as shown in Figs 2c and 2d

2) *AB*(2) is the parameter representing the line integral along *BC* (Fig 2d) and can be expressed as,

$$AB(2)=(\sigma_{yz}\ PP+\sigma_y\ QQ+\sigma_{yz}\ RR)\ 1/4 \tag{13}$$

3) If the integral

$$\int_{A(\mathrm{element})}(\sigma_{i3}u_{i,1})_{,3}\mathrm{d}A$$

of each element is denoted by *ABCM* then using the dif ference method (Fig. 2e)

$$ABCM=(ABC)'-ABC$$

where

$$ABC=(\sigma_{xz}\ PP+\sigma_{yz}\ QQ+\sigma_z\ RR)\ b/4c \tag{14}$$

(*ABC*) is obtained by Eq (14) for the neighboring element, and *c* is as shown in Fig 2e

4) The parameter representing the effect of the centrifugal force is denoted by *ABC2*

$$ABC2=(A_1\ PP+A_2\ QQ+A_3\cdot RR)\ b\rho\omega^2/2$$

where *A1* *A2* *A3* are the influence coefficients of locations Under the condition shown in Fig 2f

$$ABC2=-\{-[R_0-YC(I)]\sin\beta\ PP+ZC(I)\ QQ + [R_0-YC(I)\cos\beta\ RR\}\ \rho\omega^2 b/2$$

where *YC*(*I*) and *ZC*(*I*) are the coordinates of the element centers; ρ is the density; ω is the angular velocity; and *b* is as shown in Fig 2c

5) $$WSI=[\sigma_x^2+\sigma_y^2+\sigma_z^2-2\upsilon(\sigma_x\sigma_y+\sigma_y\sigma_z+\sigma_z\sigma_x) + 2(1+\upsilon)(\sigma_{xy}^2+\sigma_{yz}^2+\sigma_{zx}^2)]\ 1/2E \tag{15}$$

where υ is the Poisson's ratio, and *E* the Young's modulus

Numerical Results for Normal Models

In order to examine the method and program, the models shown in Fig 3a have been calculated numerically by means of the finite element method. The calculation is carried out for 32 cases according to different cracks and overall sizes (semicircular surface crack and 90 deg corner crack) Dif ferent meshes and different ways to combine the four node and eight node elements have been examined The four node isoparametric elements were used in such a way that an eight node element was divided into two triangular prisms (six node), each of which was in turn divided into three four node isoparametric elements (see Fig 3b) This was done because only the stiffness matrices of the four node and eight node element had been found The purpose of this work was to find a suitable way to combine the elements and develop a better mesh scheme, subject to the limitation of the core memory capacity of the computer Not all the calculated examples are given here, only those calculated results for which the laser photoelasticity experimental results are available are presented The calculated results are shown in Fig 3c For the sake of comparison, the curves by Tracey[4] are also shown in Fig 3c for the semicircular surface crack (denoted by 1) and the 90 deg corner crack (denoted by 2) for the dimension ratio of the model and the crack (b/a, refer to Fig 3a) equal to 5 According to Pian and Morriya [5] for such a selection of b/a

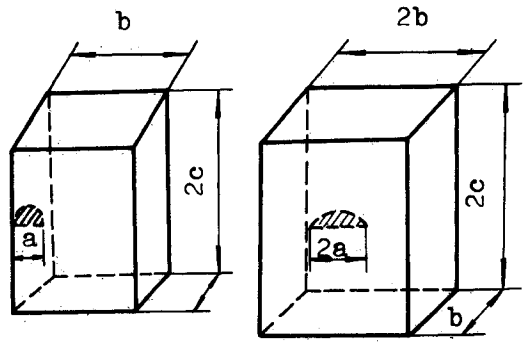

Fig 3a Calculated models

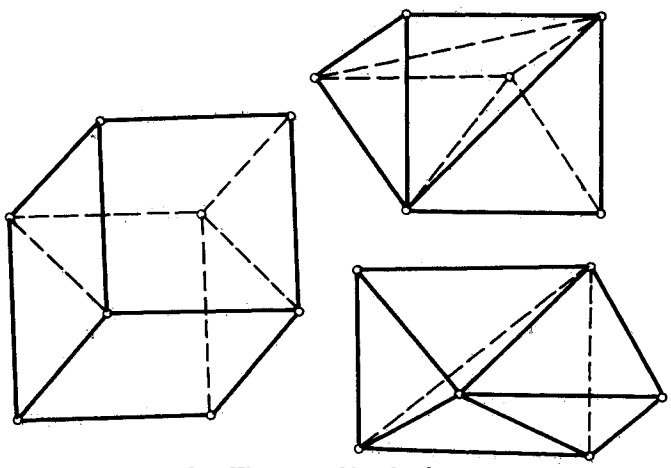

Fig 3b Way to combine the elements

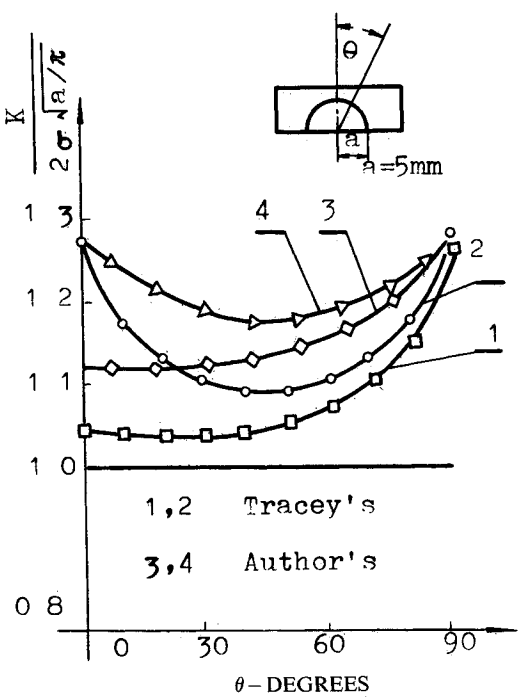

Fig 3c Comparison of results

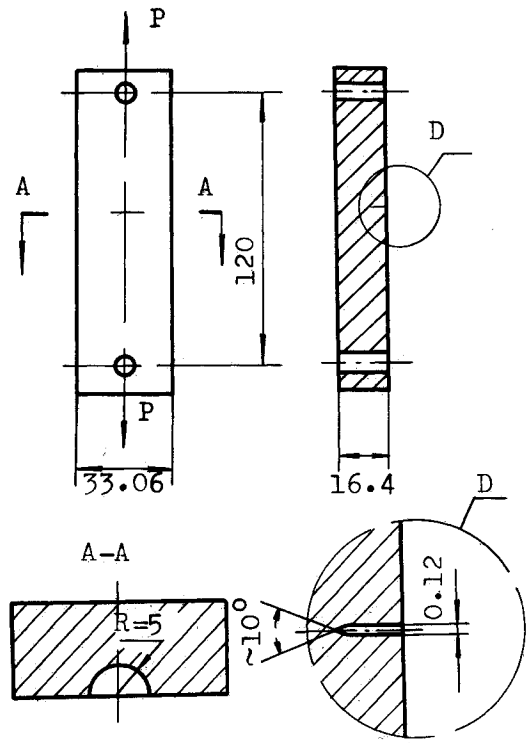

Fig 4a Photoelasticity model

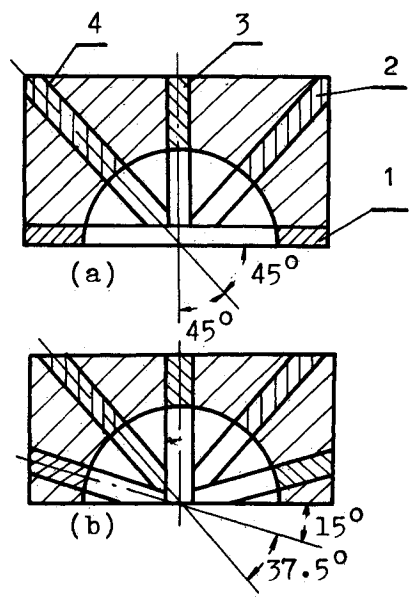

Fig 4b Cutting way

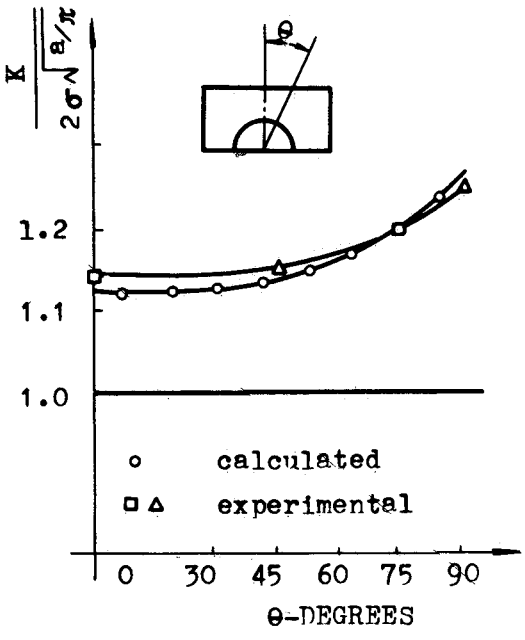

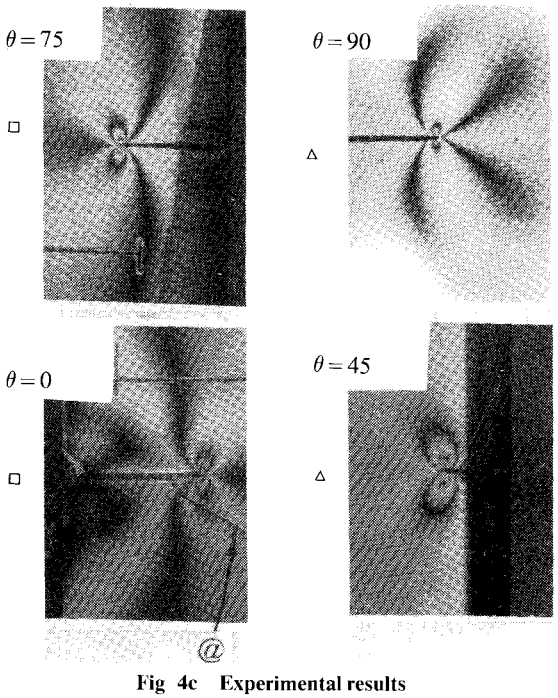

Fig 4c Experimental results

the difference between the stress intensity factors for semicircular surface cracks in a semicylinder and in a rectangular bar (even a semi infinite solid) is small The curves denoted by 3 and 4 are calculated for a semicircular surface crack and a 90 deg corner crack, respectively, by using the present method The values corresponding to some points on the curves are the average for all the paths around the point

It may be noted that the trend of the present curve agrees with that calculated by Tracey However, when $\theta = 0$ deg, the dimensionless value of the semicircular surface crack obtained in the present study is equal to 1 12 which is slightly higher than the value of 1 04 calculated by Tracey The values of the corner cracks also tend to be slightly higher because of the following reasons:

1) The dimension ratio between the model and the crack (b/a) is 3 in the present calculations but 5 in Tracey's Therefore, the effect of boundary makes the value of each point approaching the average

2) The mesh scheme created is coarser (184 nodes, 552 degrees of freedom), which will also cause certain errors

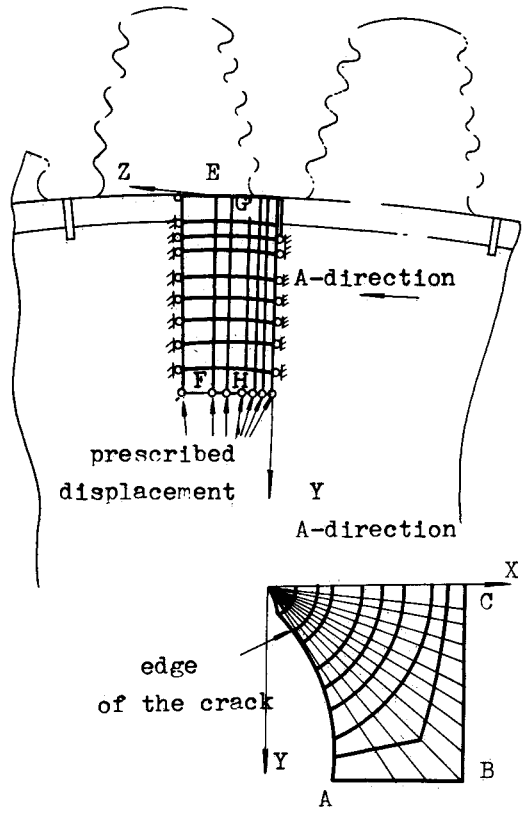

Fig 5a Model taken from turbine disk

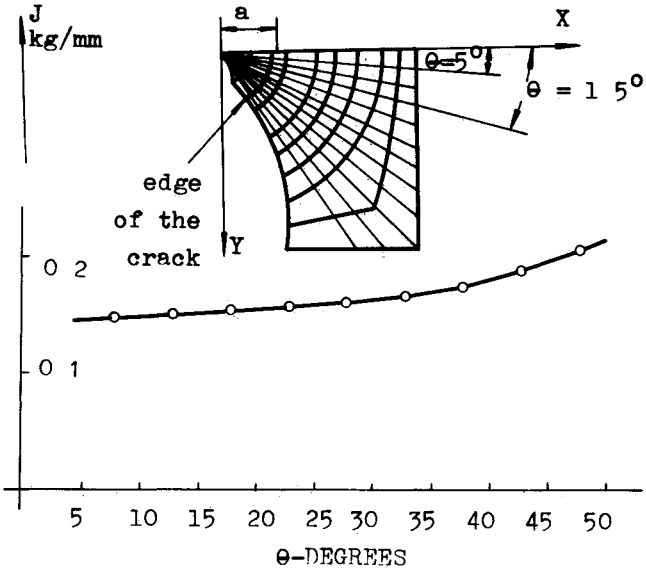

Fig 5b Calculated results of turbine disk model

Experimental Results of Laser Photoelasticity for Normal Model

The experimental model is shown in Fig 5a The crack is formed by casting a thin (about 0 12 mm) plate of steel with sharpened edge into the model made of epoxy resin 6101 The freeze temperature is 115 C The models are cut into plates in different ways to form two groups of testing models (Fig 4b) The first group is shown in the first part of Fig 4b, and the second one is shown in the second part

The experimental results are shown in Fig 4c The values of K_I are calculated from the streaks by the multipoint method [6] It can be seen that the experimental points coincide basically

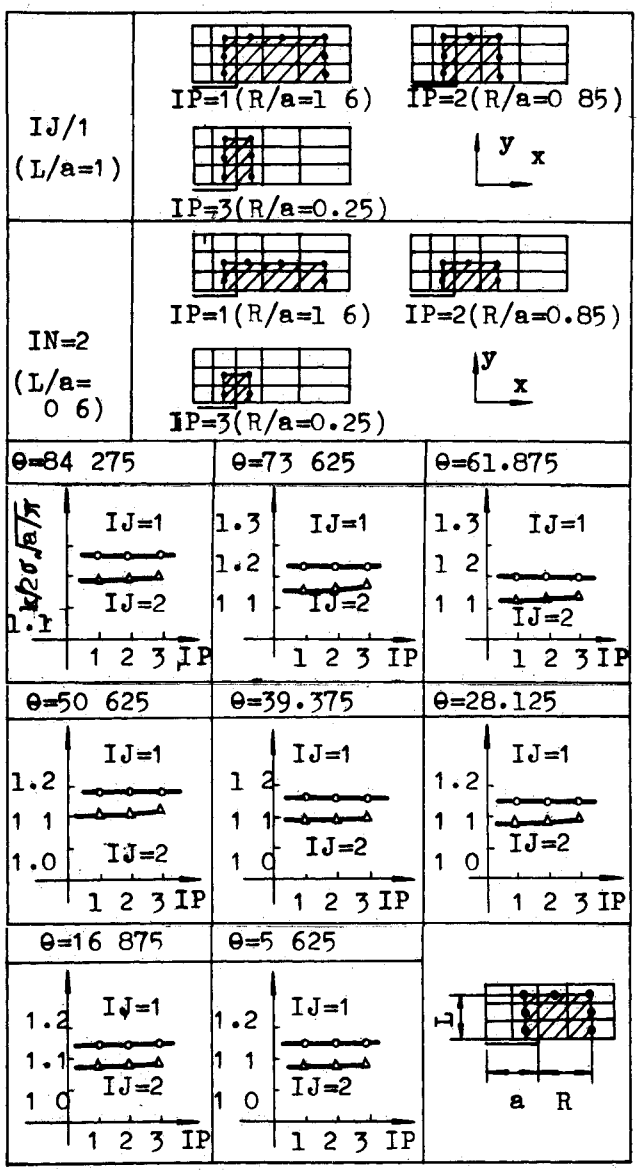

Fig 6 Invariability of integral.

with the calculated results (In the photograph at the left bottom of Fig 4c), the mark @ is a fracture due to the carelessness)

In fact, six models were cast, but only two were successfully frozen Unfortunately, a model was broken by an accident in cutting and only limited data were available

Calculated Results of a Corner Crack on the Bottom of the Fir-Tree Slot in a Turbine Disk

The "pattern model" taken from turbine disk is shown in Fig 5a. Because the core memory capacity of the computer is limited, it was assumed that on the bottom of each slot a crack exists to simplify the boundary condition

The displacement in X, Y Z directions on the lower boundary (i e AB in Fig 5a) and those in X direction on the lateral boundary (i e. BC in Fig 5a) are taken from the results calculated under the condition of axial symmetry without crack [7]

The calculated model possesses 1099 nodes and 3297 degrees of freedom The results are shown in Fig 5b It can be seen that when $a = 4$ mm and θ varies from 7 5 to 47 5 deg, the value of J varies from 0.146 to 0 205 kg/mm The rotational speed of the turbine disk is 11 500 rpm The centrifugal forces of the blades and their roots are applied on the circumference along the bottoms as a uniformly distributed load. The values of J in Fig 5b are calculated by the finite element formulas with pattern models Since the surface EF (Fig 5a) is not parallel to the surface GH, certain errors arose in the calculation For the present mesh scheme, the maximum relative error did not exceed 6% More sophisticated analysis should be carried out in the future to eliminate this error

Conclusions

1) Using ordinary eight node and four-node isoparametric elements, the present method can be readily acceptable by engineers Any familiar program could be applied to solve the stress and displacement fields Lesser time is needed for calculating the J integral of pattern model (For a pattern model containing 184 nodes, 542 degrees of freedom, the CPU time needed is only 7 minutes) In the present method two additional area integrals have been taken into account, so that the method is more general These factors persuaded the authors to study this method and it has been shown that, for the present example problems, this method is simple, ef ficient, and convenient

2) For the model shown in Fig 4a, when uniformly distributed tensile loading is applied on both ends of the model with the semicircular surface crack or corner crack (the crack is basically controlled by K_I), the effect of the first area integral is insignificant (about 2%)

3) For a three dimensional integral the path independence is proved. The J values of various paths (a single path) for the normal model are shown in Fig. 6a The θ angles are arranged in the same way as those in Fig 3c; IJ (or L/a) indicates the number of different laminates, i e., the various meshes along the y-axis (see the shaded areas at the top rows in Fig 6a); IP (or R/a) indicates the path of different meshes along the x-axis (In Fig 6a, L/a and R/a express the relative size of the mesh and the distance of the path from the crack tip to crack radius) From this figure, it can be seen that the invariability of the J integral is very good for the same angle and the same laminate But there is a deviation between the integrals on different laminates. The deviation varies with the mesh scheme When the meshes are coarse it reaches up to 12%; when they are refined it drops down to 4%

It is suggested that future efforts be directed toward the improvement of the accuracy and the perfection of the method

Acknowledgment

This study was completed under the guidance of J X Nie of the Beijing Institute of Aeronautics and Astronautics The author would like to acknowledge J A Li and the laser photoelasticity group of Beijing Institute of Aeronautics and Astronautics for their warm support and help

References

[1] Blackburn W S. Path Independent Integrals to Predict Onset of Crack Instability in an Elastic Plastic Material *International Journal of Fracture Mechanics* Vol 8 Sept 1972, pp 343 346

[2] Miyamoto H , 'Elastic Plastic Fracture Mechanics translated text Beijing Institute of Aeronautics and Astronautics Beijing China, 1980, p 124

[3] Sakata, K et al Evaluate the Intensity of the Disk Rotated Using J Integral *Transactions of the Japan Society of Mechanical Engineers* A Vol 45 No 391 (1979 3) p 237

[4] Tracey, D M. 3 D Elastic Singularity Element for Evaluation of K Along An Arbitrary Crack Front *International Journal of Fracture Mechanics* Vol 9 Sept. 1973 pp 340 343

[5] Pian T. H. H and Morriya K , "Three dimensional Fracture Analysis by Assumed Stress Hybrid Elements *Numerical Methods in Fracture Mechanics* Swansea, United Kingdom 1978, pp 363 373

[6] Zheng, G. H Chou C T and Chou Y H , The Photoelasticity Study on the Stress Density Factor of I Type Crack on the Bottom of Fir Tree Slot in a Turbine Disk BH B741 research reference, Beijing Institute of Aeronautics and Astronautics Beijing China 1979.

[7] Nie, J. X Li, C H and Nie, T , Analysis of Transient Temperature and Stress Fields in Turbine Disk and the Bottom of Its Slot ' research reference Beijing Institute of Aeronautics and Astronautics Beijing China 1980